

# We are IntechOpen, the world's leading publisher of Open Access books Built by scientists, for scientists

4,800

Open access books available

122,000

International authors and editors

135M

Downloads

Our authors are among the

154

Countries delivered to

TOP 1%

most cited scientists

12.2%

Contributors from top 500 universities



WEB OF SCIENCE™

Selection of our books indexed in the Book Citation Index  
in Web of Science™ Core Collection (BKCI)

Interested in publishing with us?  
Contact [book.department@intechopen.com](mailto:book.department@intechopen.com)

Numbers displayed above are based on latest data collected.  
For more information visit [www.intechopen.com](http://www.intechopen.com)



---

# Adaptive Coding, Modulation and Filtering of Radar Signals

---

Moutaman Mirghani Daffalla and  
Ahmed Awad Babiker

Additional information is available at the end of the chapter

<http://dx.doi.org/10.5772/intechopen.71542>

---

## Abstract

In this chapter, some of the issues associated with radar signal processing are highlighted, with an emphasis on adaptability. Signal processing operations are carried by systems in order to enhance the received signal or to clarify its content of information. Received radar signal should be subjected to processing prior to the extraction of useful target information out of it so as to emphasize desired signal among other accompanying signals. Processing of the radio frequency (RF) signal is generally done in an analogue manner, while digital signal processing (DSP) became dominant in the intermediate-frequency (IF) and low-frequency portions of the system. Since the detectability and immunity against interference and clutter strongly depend on the waveform used, it will be more efficient to apply a diverse waveform instead of confinement to an invariable waveform of a fixed code and pattern. Adaptive coding, modulation and filtering of radar signals provide high degree of diversity as well as flexibility and agility for signal processors versus changing sources of interference and environmentally dependent reflectors. Constant false alarm rate (CFAR) is an adaptive processing technique that reduces noise and clutter. Different methods are applied in CFAR technique to adaptively cope with varying clutter density and distribution.

**Keywords:** filtering, coding, waveform, modulation, adaptive, CFAR

---

## 1. Introduction

Radar signal processing is essential in a radar receiver as it is required to enhance and detect received echo signals that are immersed in noise and clutter. The waveform of the transmitted signal plays a distinctive role in the performance of the radar receiver to distinguish valid echo signals from interfering random or hostile received signals. In addition to enhancing the signal-to-noise ratio (SNR) of received signals, receiver needs to enhance the signal-to-clutter ratio (SCR) so as to increase the radar detectability of targets inside the severe clutter. The performance of the radar is highly affected by the level of the interfering signals that share

---

with the radar signal the same channel. It is affected by the unintentional interference from adjacent channels, environmental and industrial noise sources and the system noise that is generated within the elements of radar system itself.

In military applications, radar is affected as well as by intentional interference or jamming caused by others to deteriorate the ability of the radar to detect hostile targets. Increase in noise and interference lowers the signal-to-noise ratio and thus allows the false alarms rate (FAR) at the receiver output to increase. Wideband jamming signals which have already enough power may find the chance to totally saturate the receiver channel to the extent that the radar might become useless. One of the drawbacks of pulse radar is its relatively large receiver bandwidth, which adds more noise and interference. Such a large bandwidth is required to pass the narrow radar pulses with satisfactory distortion. However, filtering that reduces receiver bandwidth broadens the pulse and causes distortion, which, as well as noise and interference, deteriorate the range resolution and accuracy of the radar. This disadvantage of pulse signals makes continuous wave (CW) radar signals, which require a smaller bandwidth, more preferable within heavy jammed environments. A narrowband interfering signal affects both CW and pulse radars and does not need a large bandwidth to penetrate through the receiver; however, it needs higher power to contest with the desired radar signal.

In addition to noise and interference, the radar suffers from other types of signals which are known as clutter signals. Clutter is any unwanted object that reflects radar signals and will be shown on the radar display, together with the real targets. In air traffic control radar, both fixed and very slow moving objects are considered as clutter and need to be filtered out, so as to not reach the receiver output. There are many radar signal processing techniques that are used to reduce the clutter, such as constant false alarm rate techniques that serve in the reduction of both interference and clutter problems. Doppler processing techniques, such as the long-established moving target indication (MTI) and moving target detection (MTD), are also used to process cluttered radar signals.

## 2. Filtering of radar signals

Signal filtering means the processing of signals by altering their behaviour in the frequency domain, mostly to reject lower and higher frequency interfering signals. In general, in order to use filters to enhance SNR, bandpass filters (BPFs) process passband signals, while low-pass filters (LPFs) are used to process baseband signals, namely video signals. On the other hand, high-pass filters are used in Doppler processing to enhance demodulated video signals due to reflections that come back from moving objects. **Figure 1** demonstrates the frequency response of a typical BPF.

From the spectral analysis of pulse radar signal, it could be noticed that most of the pulse energy is concentrated on the main lobe centred about the carrier frequency. North [1] suggests the reciprocal of the pulse width as the optimum value for the bandwidth of the LPF used to process radar signals in the presence of white noise. The signal-to-noise ratio at the input of the filter can be expressed as the signal power to the average thermal noise power:

$$\text{SNR} = \frac{S}{N} = \frac{S}{kTB} \quad (1)$$

where  $k$  is the Boltzmann's constant that equals  $1.38 \times 10^{-23} \text{ JK}^{-1}$ ,  $T$  the temperature in Kelvin and  $B$  the bandwidth of the system in Hz. By substituting  $B$  with the optimum bandwidth suggested by North, we get

$$\text{SNR} = \frac{S \tau}{k T} = \frac{E}{N_o} \quad (2)$$

where  $E$  is the pulse energy and  $N_o$  is the single-sided noise density in W/Hz. This signal-to-noise ratio which is directly proportional to the energy of the signal is sometimes known as the detectability factor [2], which is defined as the minimum SNR at the output of a filter that is matched to the signal. Generally, microwave circuits and transmission lines are still being used to realize filters in the radio frequency (RF) stages, while passive LC and crystal filters were used within the intermediate-frequency (IF) stages. Other passive elements, such as surface acoustic wave (SAW) devices, have been employed in many radar receivers as bandpass filters and for other purposes [3]. However, digital signal processing (DSP) is often applied in IF and baseband stages of the radar in order to accomplish the processing of IF and video signals. Nevertheless, DSP is gradually moving towards RF.

Due to the rapid growth in the fabrication of digital processors and analogue-to-digital converters (ADCs), digital filters today are widely utilized in the IF stages for bandpass filtering

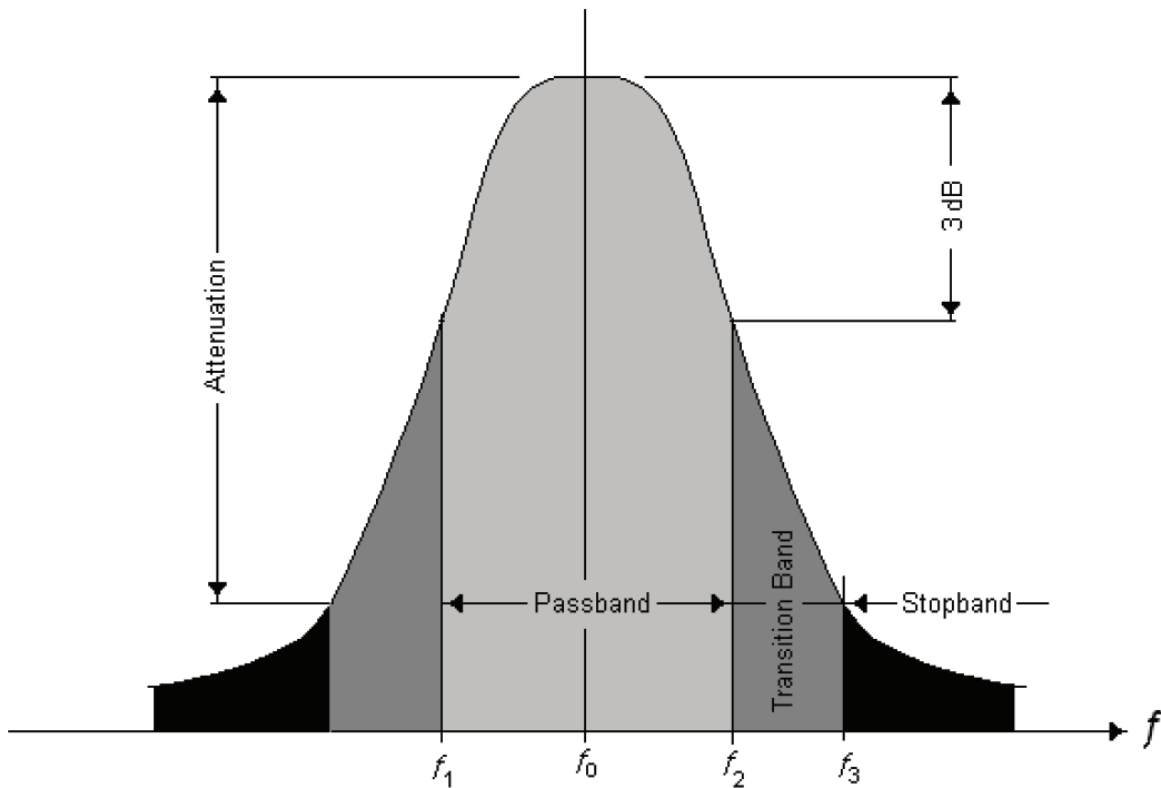


Figure 1. Frequency response of a BPF.

and other radar signal processing schemes. Both finite impulse response (FIR) and infinite impulse response (IIR) filters are used to filter IF and video radar signals [4]. For the FIR filter shown in **Figure 2**, the current sample of the output signal  $y(n)$  can be computed as the sum of the present sample of the input signal  $x(n)$  and the samples prior to it, multiplied by the coefficients of the filter  $b_k$  as

$$y(n) = \sum_{k=0}^{N-1} b_k x(n-k) \quad (3)$$

where  $N$  is the number of taps or filter coefficients.  $N-1$  is the filter order, which equals the number of delays marked as  $Z^{-1}$ . FIR filters are stable for all values of coefficients, which makes them more suitable to be adaptive. Also, they can be designed to have a linear phase response, unlike IIR filters that have a nonlinear phase response and might be unstable.

The design of an FIR filter involves finding the coefficients  $b_k$  which are the samples of the filter impulse response  $h(n)$ , which results in the frequency response that suits the required filter behaviour. An ideal LPF has an impulse response (kernel) that is proportional to the *Sinc* function, which extends to infinity. The convolution of any input signal with that impulse response shall produce perfect low-pass filtering. Nevertheless, the *Sinc* function has to be truncated in order to have an impulse response of a finite length. Because of truncation, the frequency response of the real filter will involve ripples as well as slower transition band, that occur because of the discontinuity that arises at the end of the truncated *Sinc* function. An increase of samples of  $h(n)$  will not eliminate these deficiencies because discontinuity is of a key effect. A number of windows are formulated in order to reduce the side lobes that occur because of rectangular windowing [5]. For instance, for a filter kernel of length  $N$ , the Hamming window is

$$\text{win}(n) = 0.54 - 0.46 \cos\left(\frac{2\pi \cdot n}{N}\right) \quad \text{for } 0 \leq n \leq N-1 \quad (4)$$

The design of a windowed FIR filter is based on two parameters: the bandwidth, or cut-off frequency, and the length of the kernel,  $N$ . The bandwidth is set as a fraction of the sampling frequency  $f_s$  and has a value from 0 to 0.5 (i.e. the folding frequency). Kernel length  $N$  sets the roll-off using the estimate  $N = 4/BW$ , where  $BW$  is the transition bandwidth, measured from where the curve just departs from 1 to where it is about 0. The transition bandwidth is also set as a fraction of the sampling frequency, in the range 0–0.5.

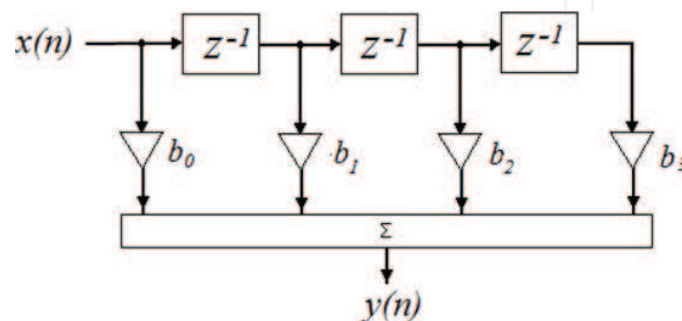


**Figure 2.** Structure of the FIR filter.

### 3. Matched filtering

We discussed the role of filters in shaping the frequency response of the receiver channel and the reflection of that on the reduction of the white noise signals. Such filtering is less effective with interfering signals that share the same band with the radar signal, that is, the passband of the filter. A filter that is matched to a signal is the one whose impulse response is a time-inverted delayed replica of that signal [6]. Thus, for a transmitted signal  $s(t)$ , the impulse response of the filter matched to the transmitted signal will be a delayed time-inverted replica of  $s(t)$ , that is,

$$h(t) = s(t_o - t) \quad (5)$$

where  $t_o$  is the optimum sampling moment. In its discrete form, for a matched FIR digital filter, its impulse response for a discrete signal of length  $N$  is expressed as

$$h(n) = s(N - n) \quad (6)$$

If we consider the response of the matched filter (MF) in the frequency domain, we will find that the transfer function of that filter is the complex conjugate of a delayed replica of the signal or a scaled value as

$$H(f) = K S^*(f) e^{-j2\pi f t_o} \quad (7)$$

The abovementioned equation indicates that the filter will be matched to waveform of the signal represented by its spectrum  $S(f)$  rather than its amplitude or time of its arrival. When we decide on using matched filtering for the processing of signals, we must carry with us that the signal will be distorted. The idea is to maximize the signal-to-noise ratio at the output of the filter prior to detection rather than preserving the original waveform of the signal. In most of the cases, it will be difficult or impossible to realize the filter of a specific transfer function that is proportional to the signal spectrum conjugate. Thus, special waveforms are to be designed to accomplish certain functions, such that the corresponding matched filters are realizable and practical. For further reading, the subject of radar signal waveform design is explained in detail in [7].

From [1, 4], it is derived that a matched filter can be realized with the aid of a correlator. This is because the output signal of a filter matched to the transmitted signal is proportional to the autocorrelation function (ACF) of the transmitted signal or a delayed replica of it, as follows:

$$y(t) = R_{ss}(t - t_o) \quad (8)$$

This conclusion states that if the received signal was free of noise, the signal at the MF output would be the autocorrelation function of the transmitted signal. If the received signal was affected by the presence of any form of noise, the output signal will be the cross-correlation function of both signals. Due to the lack of correlation between the transmitted signal and noise, the effect of noise will be dramatically reduced in the output. **Figure 3** demonstrates the use of a correlator in the processing of radar signals. The output signal at the output of a digital

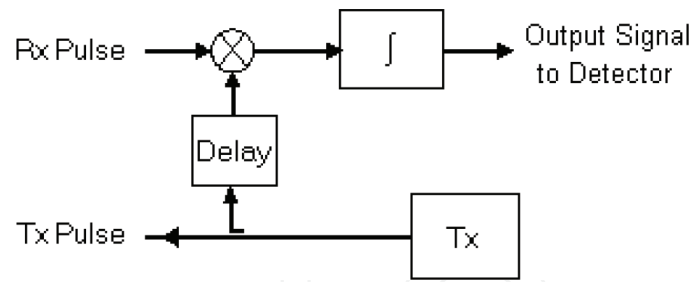


Figure 3. Correlator as MF.

MF could be either expressed as convolution between the received signal and the impulse response of the MF given in Eq. (6) or as correlation between the received signal and a delayed version of the transmitted signal like that shown in **Figure 3**, according to:

$$y(n) = h(n) * x(n) = \sum_{k=-\infty}^{\infty} h(k)x(n-k) \quad (9)$$

$$y(n) = R_{sx}(n) = \sum_{k=-\infty}^{\infty} s^*(k)x(n+k) \quad (10)$$

#### 4. Doppler filtering

Doppler filters are applied in the processing of radar signals in order to remove fixed targets and raise the signal-to-clutter ratio. There are several processing techniques to enhance the SCR in pulse radar, such as moving target indication used in the short pulse radar and moving target detection that is used in the pulse Doppler radar [2]. CFAR that will be discussed in detail is another signal processing technique that improves detection of targets inside clutter. If the wavelength of radar signal is  $\lambda$ , the Doppler frequency shift in the signal received from a target moving with a relative velocity  $v_r$  (to or from the radar) is given as

$$f_d = \frac{2v_r}{\lambda} \quad (11)$$

MTI filters are easier to be implemented and cost less compared to MTD processors. For a video signal, the MTI filter is a high-pass filter used to filter out signals of fixed targets, which is of zero Doppler frequency, and weakens signals reflected by slow targets. The MTI filter is a discrete analogue or digital filter. Therefore, it has a periodic frequency response that repeats each multiple of the sampling frequency, that is, the pulse repetition frequency (PRF) of the pulse radar. Hence as seen in **Figure 4**, an MTI filter will reject more than one moving target of the Doppler frequency that is not actually zero. Those rejected targets are of frequencies that are multiples of the PRF, which are due to targets having blind speeds that are not sensed by the radar, that is, it will be blind and will not detect those targets. Substituting PRF in Eq. (11), the first of those blind speeds is related to the PRF and the wavelength as

$$v_B = \frac{PRF\lambda}{2} \quad (12)$$

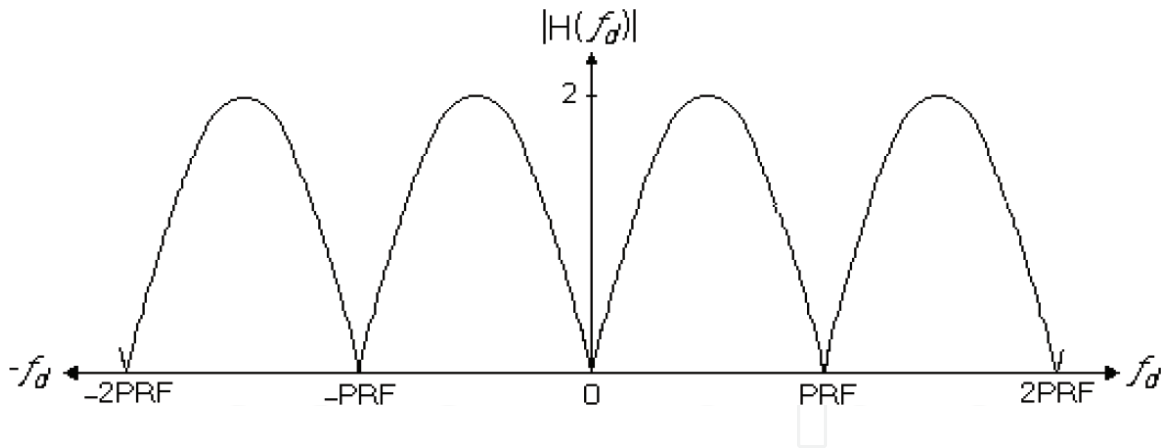


**Figure 4.** Frequency response of the MTI filter.

The MTI filter will act as a proper HPF only within the Doppler frequency range  $-PRF/2 \leq f_d \leq PRF/2$ , as illustrated in **Figure 4**, where  $f_d$  is the Doppler frequency of the echo signal, as defined in Eq. (11). That complies with the Nyquist rate that restricts  $f_s \geq 2 f_d$ , where  $f_s$  is the sampling frequency. For targets of higher Doppler shifts, velocity ambiguity occurs. A solution to avoid blind speeds difficulty is to use a staggered PRF instead of a fixed PRF. Accordingly, the probability that a target is in motion with one of the blind speeds is significantly reduced [6]. For the pulse Doppler radar that applies MTD processing, a bank of Doppler (i.e. MTI) filters is used to realize a more dynamic range in the Doppler domain. The use of this technique avoids rejection of moving targets that have blind speeds and will minimize the ambiguity in the measurement of target velocity.

MTI filters are frequently designed as FIR filters. Two-pulse canceller is a first-order FIR filter of filter coefficients  $b = \{1, -1\}$ , which is the simplest MTI filter. Higher order filters, such as the three-pulse canceller of  $b = \{1, -2, 1\}$  and four-pulse canceller of  $b = \{1, -3, 3, -1\}$ , are mostly used since they provide more flat amplitude frequency response, both in the pass-band and stopband.

## 5. Adaptive filtering

FIR filter shown in **Figure 2** is stable by definition, and hence it can easily become adaptive whatever its coefficients are. Its kernel could be modified to adapt, either to the required radar signal or to the unwanted signal due to noise or clutter [8]. For all FIR filters, the coefficients  $b_k$  are the elements of its kernel, that is, samples of its impulse response. For example, an LPF may be modified in order to reshape its frequency response according to variations of the received signal. A matched filter can be adapted to diverse waveforms that are transmitted by the radar to enhance the diversity of detection and/or to avoid some jamming signals. The MTI filter may alter the location of its notch so as to compensate for a moving radar platform, for example, an airborne MTI (AMTI) radar [2].

**Figure 5** illustrates the basic concept of the adaptive filter. The idea is to filter the input signal  $x(n)$  using an adaptive filter, such that it excels to match that signal to a desired signal  $d(n)$ . The



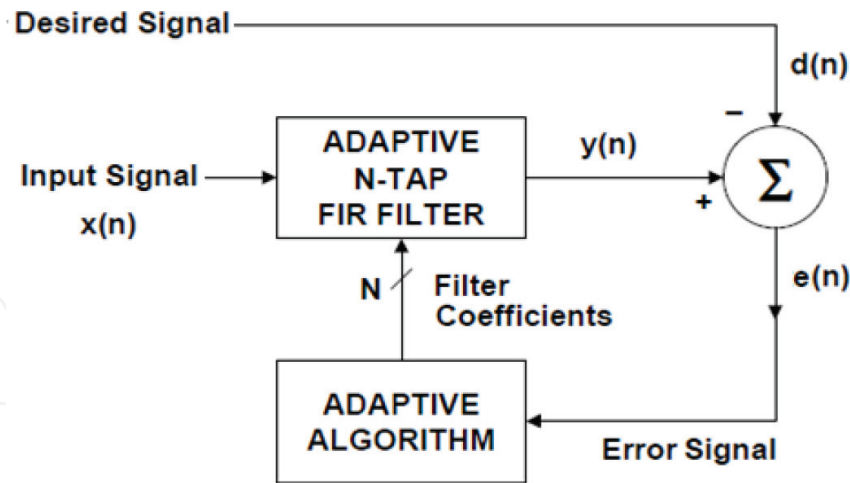


Figure 5. Adaptive FIR filter.

filtered signal  $y(n)$  is subtracted from the desired signal in order to generate an error signal. That error signal  $e(n)$  drives some adaptive algorithm, which in order generates the filter coefficients  $b_k$  in a manner that minimizes the error signal according to that adaptive algorithm. Filter coefficients are known also as tap weights  $w(k)$  of the FIR filter. Mean square error (MSE) algorithm is one of the most popular known algorithms, which in turn includes the least mean square (LMS) and the recursive least squares (RLS) algorithms [9].

In **Figure 5**, the estimation error signal at the time index  $n$  is  $e(n)$ . It is fed back to the adaptive algorithm to minimize some function of the error, known in the literature as the cost function [10]. In case of the radar, the optimal output signal of the applied adaptive filter is identical to the desired echo signal, that is, it looks like the transmitted signal. If the output signal of the filter is identical to the desired signal, the error signal becomes zero.

All MSE algorithms intend to minimize the cost function, which is equal to the expectation of the square of the difference between the current output signal of the adaptive filter  $y(n)$  and the desired signal, as follows:

$$\xi(n) = E\{e^2(n)\} = E\{[y(n) - d(n)]^2\} \quad (13)$$

LMS algorithm is generally used in adaptive filtering because of the simplicity of the required computations. It is also known as stochastic gradient-based algorithm, which makes use of the gradient vector of the filter tap weights in order to converge on the optimal Wiener solution [9]. That relative simplicity made it the benchmark versus which all other adaptive filtering algorithms would be judged. At each of the iterations of the LMS algorithm, the filter tap weights of the filter will be updated in accordance to:

$$w(n+1) = w(n) + 2\mu e(n)x(n) \quad (14)$$

In Eq. (14), the parameter  $\mu$  is the step size, which will be a small positive constant. The step size manages the influence of the updating factor. The selection of a suitable value for  $\mu$  is crucial to the performance of the LMS algorithm. If that value is so small, the time taken by the

adaptive filter to converge on the optimal solution is going to be very long. In contrast, if  $\mu$  is so large, then the adaptive filter might become unstable and thus its output signal would diverge away from the desired signal [9].

## 6. Coding of radar signal

A short pulse waveform of a single pulse is modulated only in amplitude. For the small pulse width, the range resolution is excellent and is directly proportional to that width, namely  $\delta R = c \tau/2$ . However, it will not be enough to resolve scattering targets in Doppler because Doppler resolution is proportional to the bandwidth. Bandwidth is equal approximately to the reciprocal of the pulse width and thus the time bandwidth product is about unity. Such waveforms are used in the MTI radar that uses Doppler processing just to filter out non-moving targets from its output, which does not require much better Doppler resolution.

Long pulse waveforms consist of a single pulse that is modulated only in amplitude, but now the duration will be long enough for the scattering targets to be resolved in Doppler. CW radar signals belong to this class of waveforms, with very long pulse duration. On the other hand, in a practical situation, it will not be suitable for resolving targets in range, of course unless we modulate the angle of the signal. Noise-type waveforms consist of pulses that are modulated with amplitude or phase modulation function that is irregular or noise like and has a relatively larger time-bandwidth product. This class of waveforms includes those used in pulse compression of radar signals like biphasic codes (such as Barker and pseudorandom codes), polyphase codes (such as Frank codes), nonlinear frequency modulation (NLFM) pulses, pulse trains with staggered PRF pulses, trains with frequency shift coding and long pulses with irregular amplitude modulation [7].

The radar signal is frequently coded with the purpose of pulse compression. Nevertheless, the frequency and phase coding of the radar signal are employed to accomplish other requirements rather than the compression of echo signals. Thus, the conventional pulse or CW radar signals with fixed frequencies and phase angles are not always the favourable waveforms. Nevertheless, the environment in the region of the radar includes ground clutter, multipath, refraction, weather and interference. The optimum radar signal waveform for this application must contain sufficient energy to achieve detection on the smallest aircraft at the longest range. It must also have sufficient bandwidth to provide the necessary range accuracy and resolution and must have a duration long enough to permit velocity discrimination of targets relative to ground clutter.

Pulse compression [2], also known as pulse coding, is a signal processing practice that is intended to maximize the sensitivity and resolution of radar systems. In a pulse radar system, there are several factors that affect each of the radar functional parameters. One of these factors is the effect of the pulse width in the determination of the range resolution and accuracy. The radar range equation [1] indicates that the range is affected by the energy of the transmitted pulse, that is, its power and pulse width. Generally speaking, the ability of any radar to detect far objects depends primarily on the transmitted signal energy.

For pulse radar, energy is indicated by the average transmitted signal power, which is expressed as the peak power multiplied by the duty cycle of the transmitter. Even though the peak transmitter power could be as high as hundreds of kilowatts or even some megawatts, as pulse radars transmit very short pulses (typically in order of microseconds), the average transmitted signal power perhaps is much less than 1% of that value. Obviously, this would not be the efficient use of the available transmitter power.

Transmission of longer pulses improves the detectability of the radar as it increases the average transmitted signal power. On the other hand, just lengthening the radar pulse has the result of degrading its range resolution, because the RF pulse would be spread over a larger distance. Thus, some technique is needed to increase the average power without degradation in the range resolution and accuracy of measurement. In order to solve this dilemma, we have to understand that the range resolution of the pulse radar does not essentially depend on transmitted pulse duration but in fact it depends on the bandwidth of the transmitted pulse. In old radars, a simple rectangular RF pulse is transmitted in each repetition interval. Its bandwidth is just  $1/\tau$ , where  $\tau$  is the duration. If the carrier signal within the pulse is altered using frequency or phase modulation, the bandwidth will be increased. Accordingly, the radar resolution is changed independent of the average transmitted signal power. This kind of modulation of the transmitted radar pulse is generally known as radar signal coding.

In radar signal processing, pulse compression is one of the techniques that makes use of coding to increase the bandwidth of the radar signal. At the radar receiver, reflected coded pulses are compressed in the time domain, which produces a pulse of a finer range resolution than that of an uncoded pulse. Decoding or compression involves correlating the received signal with a replica of the transmitted signal. Several methods were developed to realize that, such as binary phase and polyphase coding, frequency modulation and frequency hopping. Applying linear frequency modulation (LFM) to the transmitted pulse is often referred to as chirp coding. The main drawback of pulse compression is the appearance of range side lobes around the main signal peak after decoding. It may produce echoes that spread out from neighbouring targets and bring in range ambiguities.

A common signal coding method used in the pulse radar is binary phase shift keying (BPSK), which involves repeatedly flipping the phase of the RF signal within the duration of the pulse, according to a code known as the spreading code, which should yield minimum side-lobe levels after decoding. Barker codes are efficient binary codes, which have lengths of up to 13 bits [2] only. Side lobes can be minimized by the use of complementary codes, which are carefully selected pairs of codes whose range side lobes cancel out under ideal conditions. Generally, the efficiency of a particular code is judged by the time-bandwidth product,  $BT$ , where  $B$  is the pulse bandwidth and  $T$  is the entire transmitted pulse width. To realize a higher compression ratio, more subpulses of  $\tau$  width are used per one long pulse of  $T$  duration. For an uncoded pulse,  $BT = 1$ , as  $B = 1/T$  only.

For example, a 13-bit Barker code has a time-bandwidth product of 13, which means that each radar pulse contains 13 times the energy of an uncoded pulse of the same resolution. Range resolution becomes 13 times finer than that for an uncoded pulse of the same width. A pulse Doppler radar compromises between range and velocity resolution by applying relatively

longer pulses, while some radar systems focus on the issue of range resolution more than other parameters. Precise target tracking, range finders, target recognition and radar imagery applications are examples of those areas of interest. Synthetic aperture radar (SAR) is widely used for radar imagery and mapping and for space and aerial reconnaissance, which requires superior range resolution [3].

Pulse compression is the solution that solves almost all those problems mentioned. It makes use of specific radar signal processing techniques to provide most of the advantages of very narrow pulses yet retaining long range with less power. Matched filters, similar to those discussed in Section 3, are used to perform pulse compression of the received signals. Compression is needed because radar signals are usually expanded in time before transmission and must be compressed to obtain the desired resolution or sharp focusing. This will enhance extensively the received signal SNR and thus improve the radar detectability of far and small targets immersed inside noise and clutter. We can briefly state the merits of the pulse compression mentioned above in addition to others as follows [7]:

1. Large compression ratio offers higher resolution and accuracy in range and reduction in the radar minimum range.
2. The reduction of the required receiver bandwidth and thus reduction of interference.
3. The improvement of the SNR of the received signal due to matched filtering or correlation of signals.
4. Better anti-jamming capabilities, low probability of intercept (LPI), low probability of exploitation (LPE) and low power that makes the radar system difficult to be detected or positioned.
5. Long transmitted pulses cause low interference to other radar and communication equipment and thus provide better electromagnetic compatibility (EMC).
6. Ease of using solid-state transmitters and small power supplies like batteries that leads to small and light systems.
7. The Doppler information in the long pulse received back from a target will be richer than what is gained from a short pulse.
8. Pulse compression realizes radar imagery and mapping in addition to the possibility for target recognition and classification, using a high-range resolution (HRR) radar.

There are many techniques used in pulse compression that are generally divided into passive and active techniques, which include frequency modulation and phase modulation techniques.

## 7. Phase coding of signals

In this technique of pulse compression, the phase angle of the transmitted radar pulse is switched between two or more values, while the long pulse is modulated with the radar PRF

as usual. The relatively long transmitted pulse is divided into an integer number of subpulses, of equal widths and amplitudes but with different phase angles.

A digital signal or a code sequence is used to determine the phase of each subpulse. It is more common to use binary or biphase coding [11] to provide the modulated pulse rather than the ternary, quaternary or higher coding of signal. A signal multiplier may be used to obtain the binary phase shift keying signal that has a phase angle that swings between 0 and 180°, according to the modulating digital signal. In **Figure 6**, such a BPSK modulated pulse is illustrated. Due to the modulation of the carrier of the transmitted signal with the digital signal, the bandwidth of the transmitted signal is increased. The spreading of the digital signal in most cases is a pseudorandom signal that has special desirable correlation features. Such signals look like white noise, which has an infinite bandwidth and an infinitesimal autocorrelation function centred about the zero axis. Those pseudo-noise (PN) binary codes are used in spread spectrum communication systems, in a similar manner, in order to spread data signals along the frequency domain. They can be easily generated with the aid of shift registers (D-type flip flops) and logic circuits.

After the phase-coded signal is amplified and emitted into the radar zone of operation, the echo signal will be reflected by targets inside that zone. The received echo pulse is compressed by a matched filter or a correlator. The peak value of the compressed signal, for any code, is equal to the number of subpulses  $N$  times the pulse amplitude. The pulse width of the pulse is equal to that of the subpulse used,  $\tau$ . The pulse compression ratio (PCR) is equal to the code length, that is,

$$PCR = BT = \frac{T}{\tau} = N \quad (15)$$

Side lobes are generated within the output of the matched filter, before and after the main lobe. Those side lobes may be reduced by the selection of the proper code for the modulating signal.

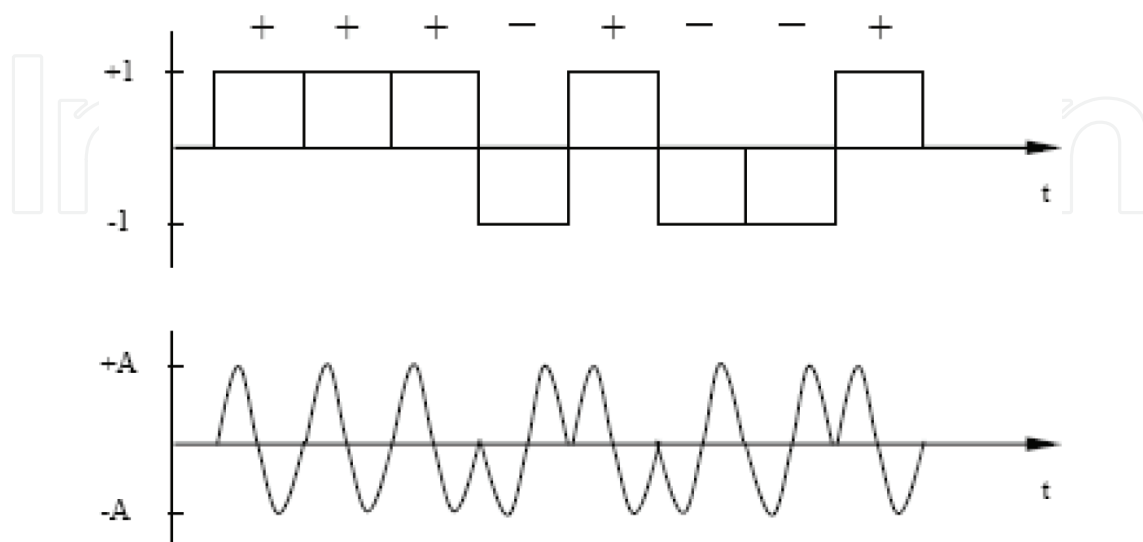


**Figure 6.** Phase-coded BPSK signal.

Many measures exist to differentiate between the available codes and decide which code is more desirable for a certain application. The features of a specific code are extracted from the ACF of the sequence that represents that code. The relations between the peak and the side lobes are of big importance. The peak-to-side-lobe level (PSL) is defined as the ratio of the largest square of side-lobe levels  $x_i$  to the square of the peak of the compressed pulse  $x_o$ , which is computed in decibels by [11].

$$PSL = 10 \log \left[ \frac{\text{Max}(x_i^2)}{x_o^2} \right] \quad (16)$$

Barker codes are one class of the famous classes of codes used in the biphase coding of the radar signal with the purpose of pulse compression. Those codes are characterized with very small PSL values and particular autocorrelation functions that have side lobes with equal amplitudes and unity absolute value, similar to that shown in **Figure 7**.

Barker codes exist for only certain code lengths that are limited to a maximum code length of 13 bits. **Table 1** shows all the available Barker codes, where a plus sign represents +1 and the minus represents -1 bit. We notice that for any of these codes, there exist four allomorphic codes that are formed by the inversion of the bits and/or the reversal of their order. All these allomorphic codes will have the same autocorrelation function, and thus we consider only one of them. The autocorrelation function of a discrete bipolar signal, that is, of '+1' or '-1' values, is approximated using the discrete temporal aperiodic ACF given as

$$\Phi(m) = \sum_{k=1}^N x_k x_{k+m} \quad (17)$$

where the integer index  $m$  steps over the domain  $-(N - 1) \leq m \leq (N - 1)$  and  $x = 0$  for all indices  $k < 0$  and  $k > N + 1$ .

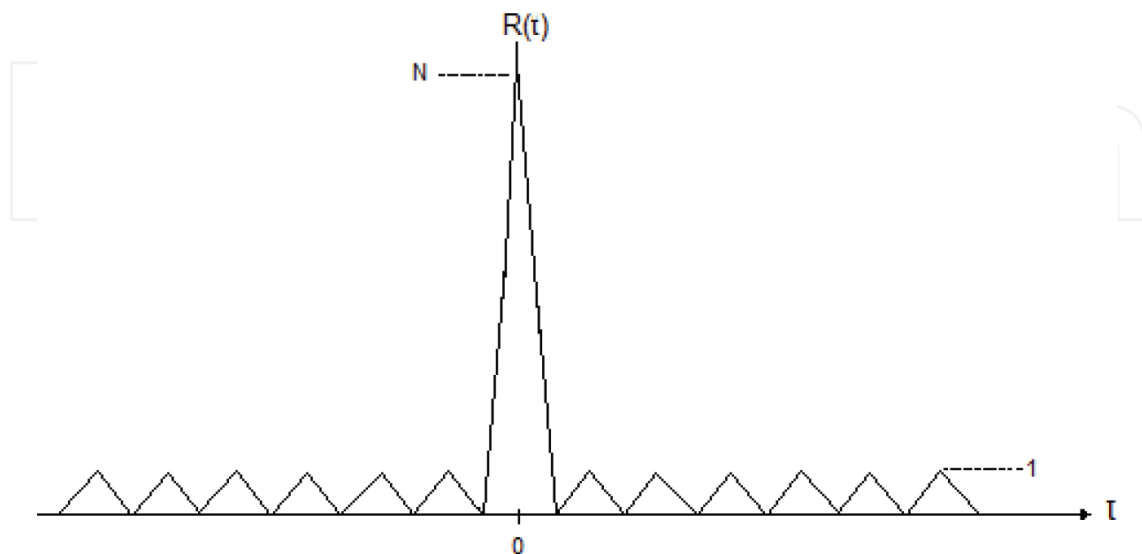


**Figure 7.** ACF of 13-bit Barker code.

| Code length | Code sequence           | PSL, dB |
|-------------|-------------------------|---------|
| 1           | +                       | -       |
| 2           | + -, ++                 | -6      |
| 3           | ++ -                    | -9.5    |
| 4           | ++ - +, +++ -           | -12     |
| 5           | +++ - +                 | -14     |
| 7           | +++ - - + -             | -16.9   |
| 11          | +++ - - - + - - + -     | -20.8   |
| 13          | +++++ - - - + - - + - + | -22.3   |

**Table 1.** List of Barker codes.

Barker codes are a subset of other binary codes known as the minimum peak side lobe (MPS) codes that attain the lowest PSL for a given code length. Thus, we find that many approaches to finding binary sequences with good side lobes have been undertaken. By means of an extensive computer search, binary codes of long lengths can be found. According to [11], Delong has discovered a considerable number of these codes as long as 99 bits with a peak side lobe amplitude of 7. And according to [7], Kerdock later has built a dedicated computer and has applied it successively to search for good codes. However, neither of them has made any attempt to ascertain that the discovered codes are MPS nor have they compiled a list of all codes of a given length with a given PSL, although long codes with excellent PSL values have been discovered this way.

There exist other approaches to achieve longer codes providing higher pulse compression ratios but look different somewhat from Delong and Kerdock approaches. One of these is the process of code concatenation or combination, in which available codes are utilized to code the transmitted pulse at more than one level; thus, each segment of the code is coded again with another phase code. When utilized with Barker codes it has been called Barker-squared or combined Barker coding. Referring to [11], Hollis combined a Barker code of length 4 with the code of length 13 in two ways, each of different ACFs.

## 8. Pseudorandom codes

A random code is to be obtained when the binary bipolar sequence is determined by a random process, with an equal probability of 0.5 for both positive and negative values. A pseudorandom, or pseudo-noise code, is obtained when the binary sequence has approximately the same number of positive and negative values with a probability  $\approx 0.5$ .

An important class of pseudorandom codes is the maximal-length sequences or shortly the m-sequences. These sequences are known also in the literature as Galois and PN codes [7]. While Barker codes are finite, the m-sequences are not finite and can realize higher compression ratios. Periodic m-sequences are easily generated with the aid of linear shift registers and XOR gates. The register is fed back with a number of its different stages of outputs, after they

are XORed or modulo-2 summed. However, certain feedback connections of the register stages outputs to the input and not all of them will produce codes of maximal length, that is, m-sequences. The maximal length of the sequence is the longest possible period for an n-stage register, which is given in terms of the number of register stages (flip-flops) as

$$N = 2^n - 1 \quad (18)$$

A cycle of the periodic autocorrelation function of an m-sequence can be computed by Eq. (17). It is shown in **Figure 8** where it looks somehow different from the ACF of a Barker code. The ACF function might be preferred to be normalized to  $N$ , which is the peak value at  $m = 0$ . As the code length  $N$  tends to infinity and the subpulse width  $\tau$  tends to zero, the ACF of the m-sequence tends to that of white noise, which is an impulse that is centred at a zero time shift. Hence, the name PN is significant. It may be worth to remember that the power spectrum density of white noise is constant with frequency. A well-known example of white noise is the thermal noise that has a power density of  $kT_o$ , where  $k$  is the Boltzman's constant and  $T_o$  is the absolute temperature. In the absence of Doppler shift, the circular autocorrelation function has two levels. Its amplitude at the origin (i.e. for  $m = 0$ ) is equal to the length of period  $N$ . For all offsets other than multiples of one period, the magnitude of the function is unity. This may be written as

$$x_m = \sum_{k=1}^N a_k a_{k+m} = \begin{cases} N & m = 0, \pm N, \dots, \pm kN \\ -1 & \text{otherwise} \end{cases} \quad (19)$$

There are  $2N-1$  samples in the autocorrelation function and this function is symmetrical about the origin. PN codes are often chosen over randomly coded words for application because their generation and decoding can be easily mechanized, their side lobe levels easily predicted and they provide a rich source for good codes of arbitrary length. Pseudorandom sequences have some properties that they share with random sequences and other properties that are unique for them. The number of segments of *ones* in each period of the sequence is within one, that is,  $\pm 1$ , of the number of *zeros* (minuses), which is known as the balance property. In every period, half the runs have length 1, one-fourth have length 2, one-eighth have length 3 and so on (the run property).

PN codes can be generated deterministically through the implementation of shift registers with feedback connections. The initial condition in the shift register determines the starting point of the code. The condition of all zeros is forbidden. The last stage in the shift register must be connected to the feedback circuit and there must be an even number of feedback taps [4]. For maximal-length PN codes, each period has a length of  $2^n-1$  pulses. There are  $2^n-1$  different maximal-length codes that can be generated from each n-bit shift register, which are simply shifts of each other derived by changing the seed utilized. The number of different n-bit shift registers that yield maximal-length codes, that is, the number of codes (including mirror images), is given by

$$M = \frac{\Phi(2^n - 1)}{n} \quad (20)$$



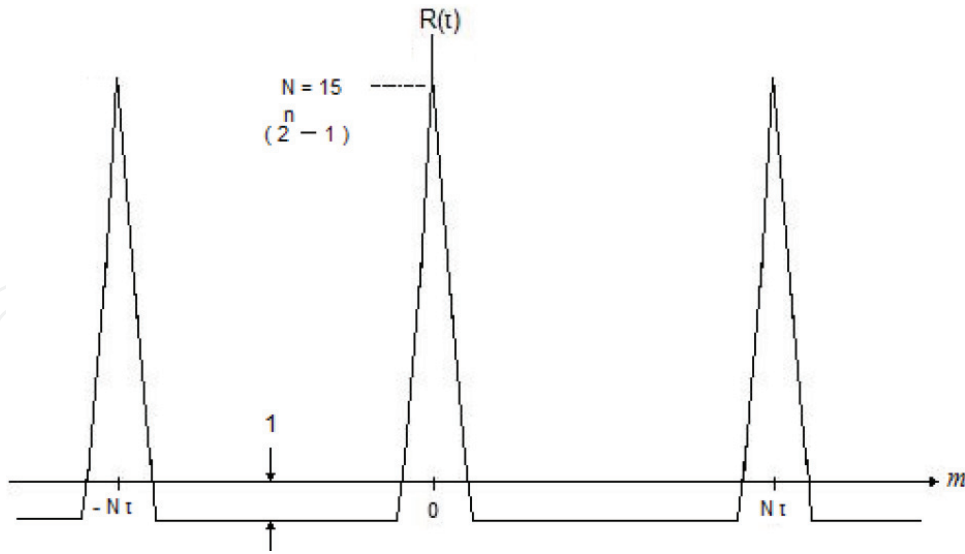


Figure 8. ACF of a 15-bit M-sequence.

where  $\Phi(x)$  here is the Euler phi function [11]. If  $2^n - 1$  is a prime number, the number of codes will be  $(2^n - 2)/n$ , whereas if  $2^n - 1$  is factorable into prime numbers denoted as  $P_i$  then

$$M = \frac{(2^n - 1)}{n} \prod \frac{(P_i - 1)}{P_i} \tag{21}$$

Each prime  $P_i$  is used in the foregoing computation only once even if it appears in the factorization more often. Algebraic sum of all the ACFs for all the starting points of a given code is  $(2^n - 1)^2$  at the origin and  $[(N - k)/N] (2^n - 1)$  for each segment,  $k$ , away from the origin, in either direction. The ACFs of this waveform is symmetrical about the time delay axis, as shown in **Figure 8**.

### 9. Adaptive coding

Diversity is a key solution for many radar and telecommunications problems. Using diverse radar elements of different parameters rather than depending on a single element enhances the radar capability and functionality. For instance, frequency diversity increases the detectability of the radar to detect different targets of different resonant sizes. Similarly, using diverse PRF reduces the problem of blind speeds in the Doppler processing of signals [7]. Earlier, most radar pulse coding was done for the sole purpose of achieving the benefits provided by pulse compression. Exceptions included the use of frequency modulation for ranging applications, for example, continuous wave and high PRF radar and the use of coded pulse trains to increase Doppler resolution. Nowadays, radar signal coding is used for other purposes such as security and waveform diversity. Waveform diversity takes many forms, including PRI diversity, frequency diversity, amplitude diversity and phase diversity.

Optimal coding is based on a certain criterion such as measurement errors, detection performance and false alarm probability. These criteria have traditionally placed certain restrictions

on code selection. For instance, the repeated use of a single pulse code meets most optimality requirements for traditional applications, and identically coded pulse trains can be used to demonstrate greatly enhanced Doppler processing [12]. On the other hand, diverse pulse coding techniques are required to ensure that target responses from individual pulses are distinguishable from one another. This inherently requires the generation of code families that possess good autocorrelation properties and cross-correlation properties as well, which are often mutually exclusive properties.

Phase-coded radar signals offer a remarkable flavour of diversity that simply depends on the change of the code of the modulation sequence. Such signals are easily generated compared to other diverse radar signals that require changing the carrier frequency. Frequency hopping signals may be considered as diverse code signals, in which its pattern of changing codes is optimized for diversity to avoid jamming, rather than to enhance the range resolution of radar. For a radar that uses a pseudorandom waveform, a comprehensive search of possible waveforms could be attempted. The choice of waveform may be reduced upon many rules, such as search of maximal-length sequences that do not include binary codes of all '1s or all '0s, which definitely do not accomplish the required resolution. Several codes are satisfactorily close that only one of a set might need to be tried. However, the number of combinations is still big, and extensive search of high time-bandwidth codes could not be practical using available computers. Nevertheless, regarding the current improvement in computer speeds, the power to do this seems to be achievable.

For example, if a correlator can correlate a waveform with 1 ms integration length in real time, it could search 10,000 waveforms in only 10 s. Therefore, if all the possible low probabilities of exploitation techniques were employed as efficiently as possible, it becomes so difficult to exploit the transmitted signal within tactical timescales. A great deal of research is being carried on to investigate waveform that designed and the related signal processing for the high-resolution pulse Doppler imaging, both in radar and in sonar.

The uncertainty association of Fourier transformation states the primary limitation on the ability of any individual waveform to simultaneously resolve two or more targets closely spaced in both time delay and Doppler shift [13]. Transmitting successive signals of adequately diverse waveforms and processing them properly could make it possible to resolve those targets and generate a high-resolution delay-Doppler image. It is somehow similar to the situation of generating a high-resolution optical image from several low-resolution optical images with somehow different imaging apertures. A selection of optimal sets of coded waveforms and designing associated processing algorithms has already been considered [13], for example, in order to generate pulse-echo delay-Doppler images of a substantially higher resolution than that is possible using a single waveform with comparable time-bandwidth product. In an adaptive diverse system, the instantaneous waveform is selected to improve the performance according to changes in clutter and noise variations [8].

The importance of this technique is based on the fact that it realizes the higher discrimination of radar or sonar targets compared to those that are possible using only one waveform. It results in higher resolution images in pulse-echo imaging systems, in addition to improved capability in resolving targets in tracking systems. There are many applications that can benefit from this superior delay-Doppler resolution, such as SAR, planetary and ground-based

astronomy radar, ionospheric radio sounding, meteorological radar, aircraft surveillance and tracking radar and in active sonar systems.

For better reduction of interference of several radar signals, one may use sort of orthogonal codes, such as Walsh codes, in same manner as in the code division multiple access (CDMA) technique used in mobile networks. However, though those codes have good cross-correlation properties that make them exceptional in multiuser environments, and they have poor PSL due to their undesirable ACF properties. On the other hand, MPS and PN codes are not orthogonal but they have very considerable PSL that realize high SNR at the output of matched filter and high-pulse compression ratio, with the minimum range ambiguity [7].

## 10. Constant false alarm rate

A major problem that encountered the performance of radar is clutter, which is defined as the unwanted targets that may compete with the desired targets in the radar receiver. There are many efforts exerted to model, analyse and mitigate clutter in radar systems. Many techniques appeared in the literature deal with modelling and filtering of clutter. Clutter is a random phenomenon and it is well described in the context of a probabilistic framework.

In this section, analysis of well-known CFAR detectors is going to be accomplished. It also includes a brief overview of topics related to clutter modelling and mitigation in the monostatic radar. Finally, the schemes of CFAR detectors under different clutter scenarios will be covered.

### 10.1. CFAR in monostatic configuration

Sometimes the clutter residue, after the moving target indicator, is enough to saturate the radar display. To overcome such shortcomings, a clutter estimation circuitry is provided after MTI to reduce the effect of false alarms. There are many schemes devised in the literature to keep the level of false alarms constant. Here in this section, an analysis of some well-matured schemes will be given. It is well known that when the radar returns come from a background with homogeneous clutter, the cell average (CA) CFAR is adequate to control the false alarms. In some cases, there will be strong returns from some targets that may mask other weaker targets. In these cases, it is better to use a clutter estimation scheme based on choosing the Smallest-Of (SO) sample of returned clutter power to represent estimation to the background clutter, which is known as SO-CFAR. In cases of clutter power transition, it is better to use a scheme based on choosing the Greatest-Of (GO) sample in the reference window as an estimation to clutter background. This scheme is known as GO-CFAR sample, as a representative to clutter.

In other situations, there may be spiky samples of the clutter in one side of the reference window, which is known as a clutter edge. Order statistic is another clutter estimation scheme that may be used to alleviate both the problem of multiple targets and clutter power transition in the reference window. In some situations, a radar receiver is encountered by a fixed position clutter during several scans. Such types of clutter can be stored and subtracted in the course of the following scans. Such clutter is called a clutter map or area clutter. In the following

paragraphs, we will give a short review to the concept of each of these schemes that is used to reduce the effect of false alarms. All these schemes are capable of setting adaptively a threshold to represent the local clutter background in the chosen reference window. The threshold in these schemes of CFAR is set on a cell-by-cell basis by processing a group of cells of a reference window sited on either side of a cell under test (CUT). **Figure 9** gives a general structure of the CA-, SO- and GO-CFAR.

### 10.2. CA-CFAR clutter estimation scheme

In this scheme, a reference window of length  $N$  cells is chosen to represent the local clutter power background. The CA-CFAR will maximize the probability of detection if the clutter background is homogeneous and of independent and identically distributed (i.i.d.) observations. As the size of the window increases, the detection probability approaches that of the optimum detector based on a fixed threshold.

The CA-CFAR makes its estimate of clutter power by summing samples of background before and after a CUT, then taking the average of them, assuming that the underlying noise distribution is homogeneous (i.e. exponentially and independent and identically distributed samples). Of course the processor will encounter severe performance degradation if the above assumption is violated. These violations may occur in terms of interfering targets or a clutter power transition (clutter edge), and in both cases a result is the unnecessary increase in the threshold and reduction in probability of detection.

In order to analyse the detection performance of a CA-CFAR scheme with the assumption that the clutter background is homogeneous, assume that the square-law detected output for any range cell is exponentially distributed with the probability density function (PDF) [14]

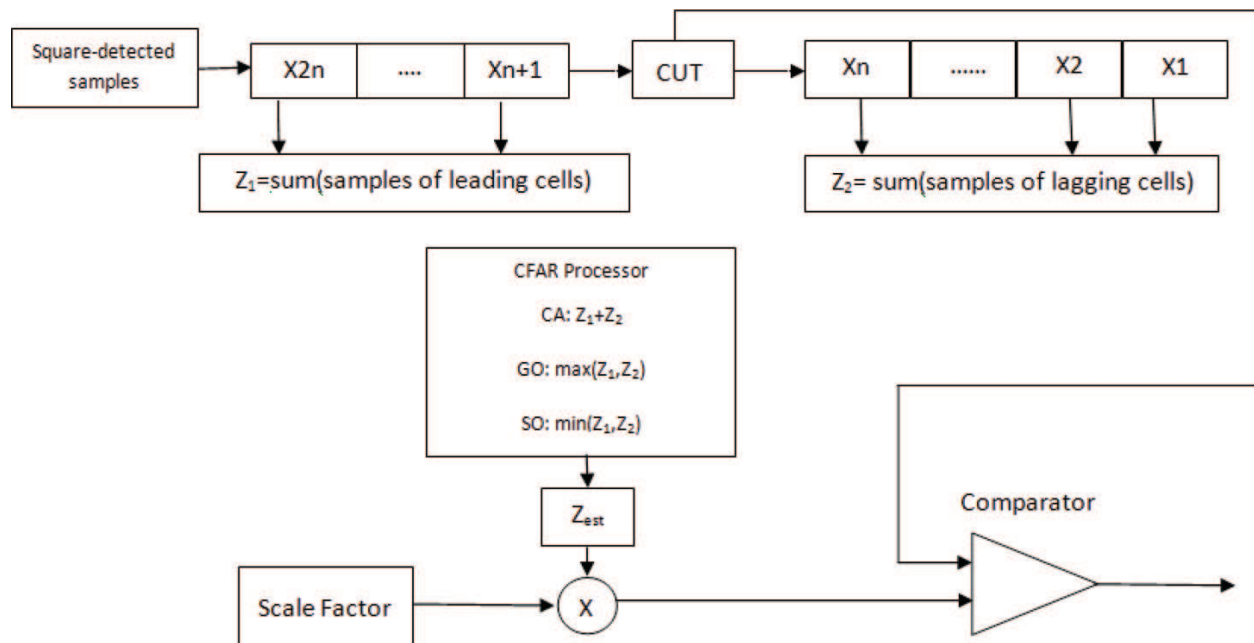


**Figure 9.** Mean level CFAR processors.

$$f(x) = \frac{1}{2\lambda'} \exp\left(-\frac{x}{\lambda'}\right) \quad (22)$$

Under the null hypothesis ( $H_0$ ) of no target in a range cell and homogeneous background,  $\mu'$  is denoted as the total background clutter plus thermal noise power, which is denoted as  $\lambda'$ . Under the alternative hypothesis (presence of target  $H_1$ );  $\lambda'$  is equivalent to  $\mu'(S + 1)$ , where  $S$  is SNR of a target. This means that we are assuming the Swerling I model for a target. Therefore, the CUT will be given as

$$\lambda' = \begin{cases} \mu' \rightarrow H_0 \\ \mu'(S + 1) \rightarrow H_1 \end{cases} \quad (23)$$

The cells surrounding CUT is always given by  $\mu'$ . The optimum detector sets a fixed threshold to determine the presence of a target under the assumption that the total homogeneous noise power  $\mu'$  is known a priori. In this case the probability of false alarm  $P_{fa}$  is given by [15]

$$P_{fa} = P[y > y_b | H_0] = \exp\left(-\frac{y_b}{2\mu'}\right) \quad (24)$$

where  $y_b$  denotes the optimum fixed threshold. Similarly, the probability of detection in the case of optimum detector is given as [15]

$$P_{dopt} = P[y > y_b | H_1] = \exp\left(-\frac{y_b}{2\mu'(S + 1)}\right) \quad (25)$$

Eqs (24) and (25) can be combined to give

$$P_{dopt} = [P_{fa}]^{\frac{1}{S+1}} \quad (26)$$

A code written in Matlab is used to present the performance of the optimum receiver in terms of SNR versus  $P_d$  with fixed  $P_{fa}$  and varying reference window length, using Eq. (26), as shown in **Figure 10**.

In the problem of setting adaptive threshold for the radar receiver to cope with the varying clutter power levels, the CFAR scheme has to follow the clutter localities. The estimate of clutter power,  $\hat{Z}$ , in this case is a random variable which is dependent on the specific CFAR scheme. It can be stated that  $P_{fa}$  is determined by the following expression [15]:

$$P_{fa} = E\left[P(y) > \hat{Z}\tilde{T} | H_0\right] = E\left[\int_{\hat{Z}\tilde{T}}^{\infty} \left(\frac{1}{2\lambda'} \exp\left(-\frac{y}{\mu'}\right)\right)\right] = E\left[\left(\exp\left(-\frac{\hat{Z}\tilde{T}}{2\mu'}\right)\right)\right] = M\left(\frac{\tilde{T}}{2\mu'}\right) \quad (27)$$

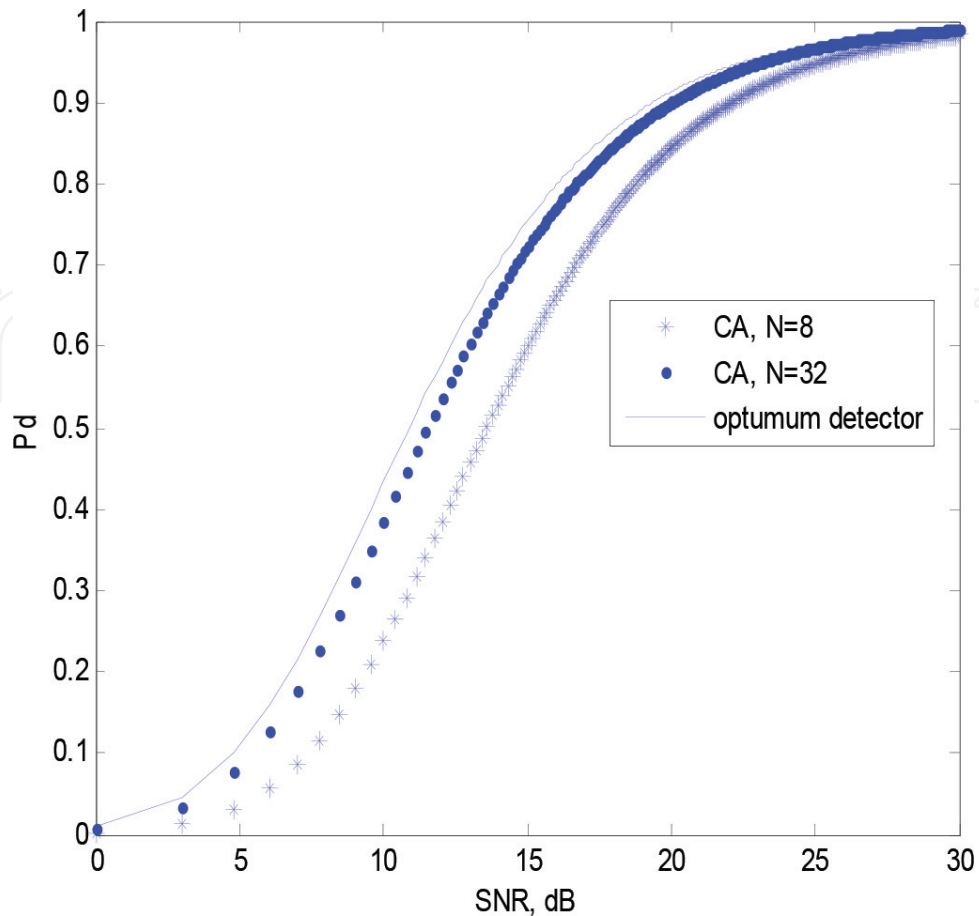


**Figure 10.** Performance of CA-CFAR with varying window length and fixed  $P_{fa} = 1e-4$  detector.

where  $M(\cdot)$  is the moment generating function (MGF). Similarly, the probability of detection can be given by [14]

$$P_d = M\left(-\frac{\check{T}}{2\mu'(S+1)}\right) \quad (28)$$

For CFAR action to hold,  $M(\cdot)$  must be independent of  $\mu'$ .

In the CA-CFAR scheme, the noise estimate is obtained by summing the power content in the reference cells before and after the CUT. This may be the adequate estimate when the background noise is exponentially distributed. Therefore, the noise estimate for this scheme can be written as

$$\hat{Z} = \sum_{i=1}^N X_i \quad (29)$$

where  $X_{is}$  are range cells surrounding CUT. The exponential density is a special case of the gamma density with  $\alpha = 1$  in the PDF given by [16]

$$f(y) = \frac{\beta^{-\alpha} y^{\alpha-1} \exp\left(-\frac{y}{\beta}\right)}{\Gamma(\alpha)} \quad y \geq 0, \beta \geq 0, \alpha \geq 0 \quad (30)$$

The cumulative distribution function (CDF) corresponding to this PDF is denoted by  $G(\alpha, \beta)$ . The moment generating function to  $G(\alpha, \beta)$  is [16]

$$M_y(u) = (1 + \beta u)^{-\alpha} \quad (31)$$

The probability detection  $P_d$  for the CA-CFAR processor is obtained by substituting Eq. (31) into Eq. (27) with  $\beta = 2\mu'$ , and  $\alpha$  is number of samples in the reference window; the following expression for  $P_d$  will result in

$$P_d = \left[1 + \frac{\check{T}}{1+S}\right]^{-N} \quad (32)$$

When setting  $S = 0$  in Eq. (32), the scale factor  $\hat{Z}$  is obtained as

$$\check{T} = [P_{fa}]^{-\frac{1}{N}} \quad (33)$$

It is clear that from Eqs. (32) and (33), that both the  $P_d$  and  $P_{fa}$  expressions are independent of  $\mu'$ , proving the action of CFAR. The performance of CA-CFAR is shown in **Figure 11** in terms of SNR versus  $P_d$  with  $P_{fa}$  as a parameter. Also, it is shown in **Figure 12** the performance of

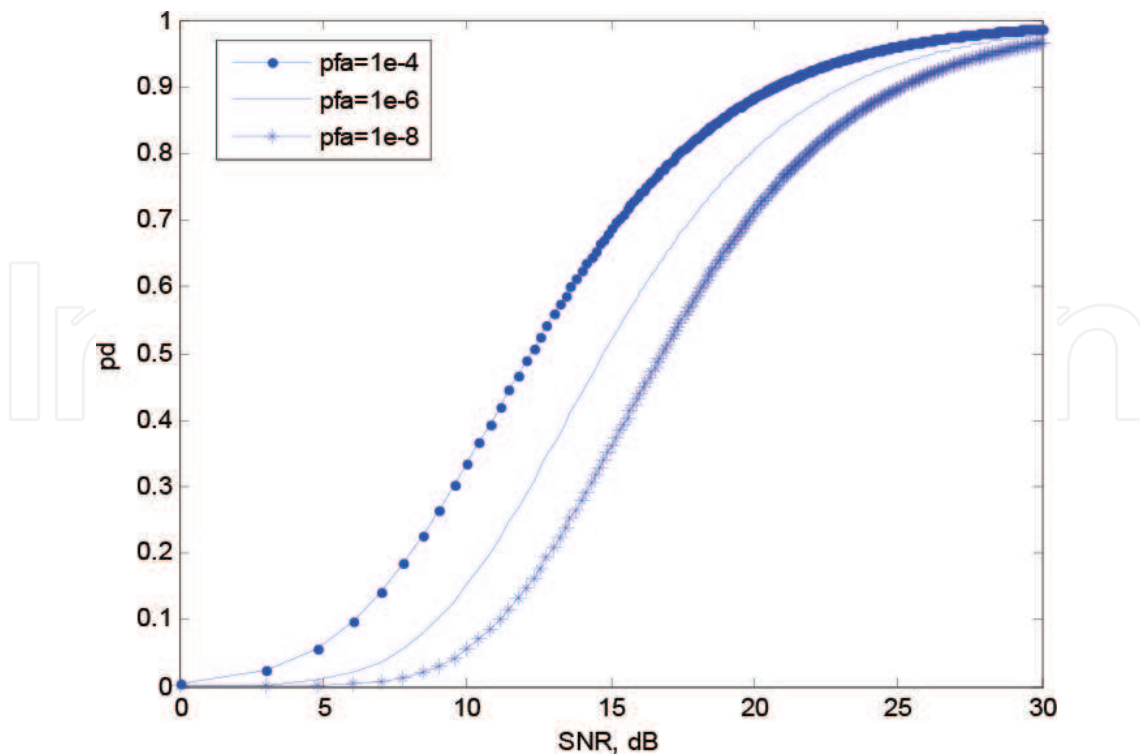


**Figure 11.** Performance of CA-CFAR.

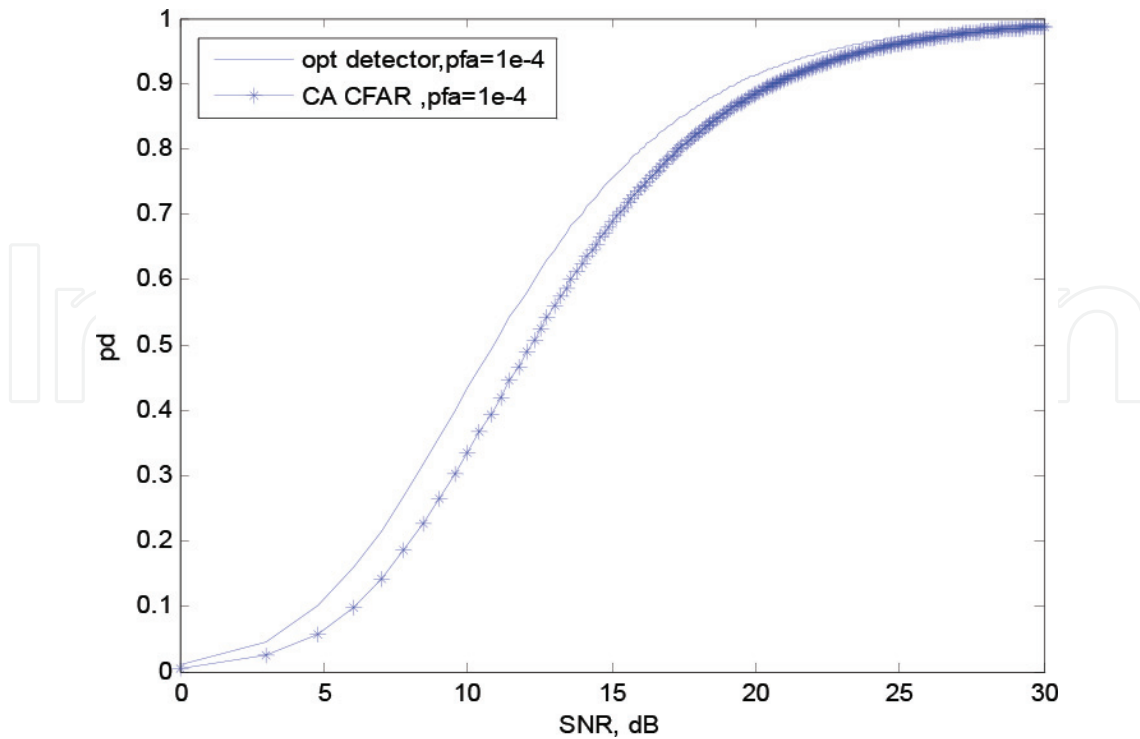


Figure 12. Performance of CA-CFAR compared to that of optimum detector.

CA-CFAR compared to the performance of the optimum detector when the designed probability of false alarm is  $P_{fa} = 10^{-4}$ .

The performance of CA-CFAR in a non-homogeneous background taken from a reference window can be analysed in similar way to the above discussion. The probability of detection obtained under CA-CFAR for this case is given as

$$P_d = [1 + (1 + I)\check{T}]^r \left[ 1 + \frac{\check{T}}{1 + S} \right]^{r-N} \quad (34)$$

where  $r$  is the number of interfering targets. Figure 13 shows the performance of CA-CFAR in a non-homogeneous environment compared to that in a homogeneous one. Also from Figure 14, it illustrates the performance of this processor when the number of interfering targets is two and probability of false alarm is  $10^{-4}$  with the reference window length as a varying parameter.

### 10.3. SO-and GO-CFAR clutter estimation schemes

Excessive number of false alarms in the CA-CFAR processor at clutter edges and degradation of detection probability in multiple target environments are prime motivations for exploring other CFAR schemes that discriminate between interference and primary targets. Candidate schemes are SO- and GO-CFAR to deal with the two problems, respectively. Here in this section, analysis of the two schemes will be given. The two schemes are modifications to the CA-CFAR scheme, and each of them overcomes one of the two mentioned problems, with the



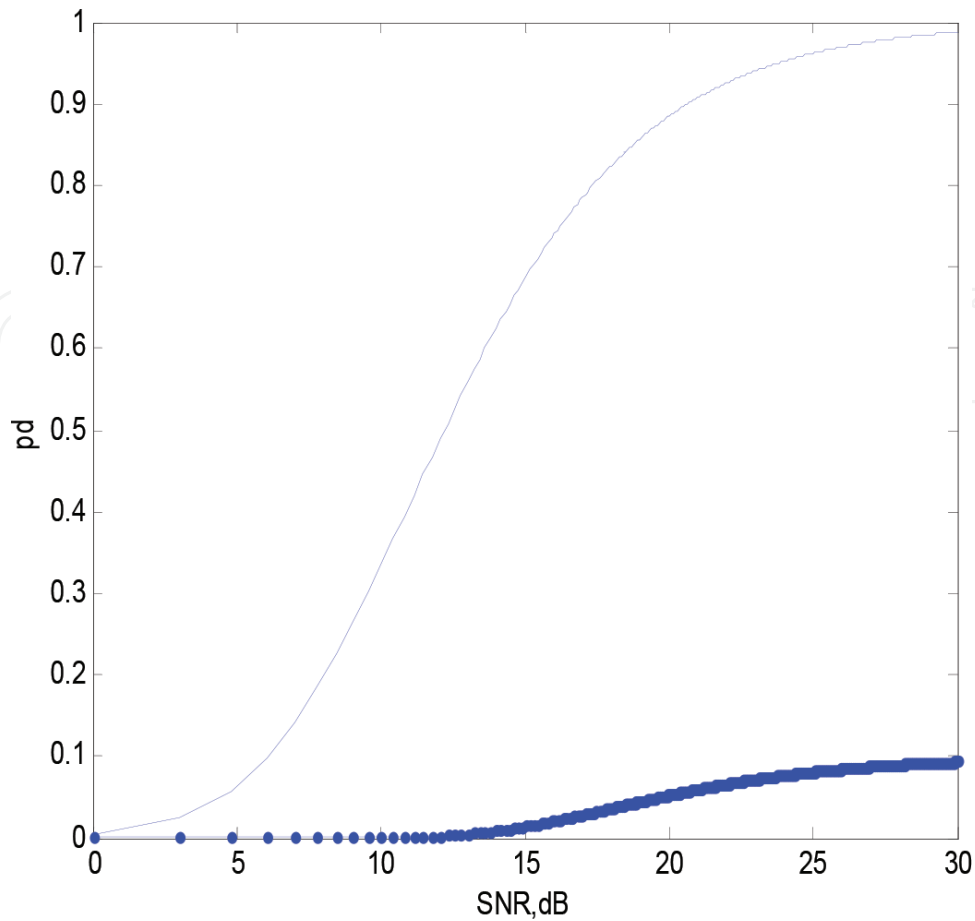


**Figure 13.** Performance of CA-CFAR processor in a homogeneous environment versus performance in a non-homogeneous environment (two interfering targets).

addition of loss of power when operating in a homogeneous background. As abovementioned, the GO-CFAR maintains the false alarms constant when the clutter edge is encountered in the reference window, while the SO-CFAR resolves the interfering targets.

A modified scheme proposed in [16] known as GO-CFAR is specifically aimed at reducing false alarms at clutter edges. The estimated total noise power is obtained from the larger of two separate sums calculated for leading and lagging reference cells to the CUT. For this scheme, we have (see **Figure 9**)

$$Z = \max(Y_1, Y_2) \quad (35)$$

where

$$Y_1 = \sum_{i=1}^n X_i$$

with  $n=N/2$ , where  $N$  is the number of tested cells. In general, the PDF of  $Z$  in (35) is given in [15] as

$$f(Z) = f_1(Z)F_2(Z) + F_1(Z)f_2(Z) \quad (36)$$

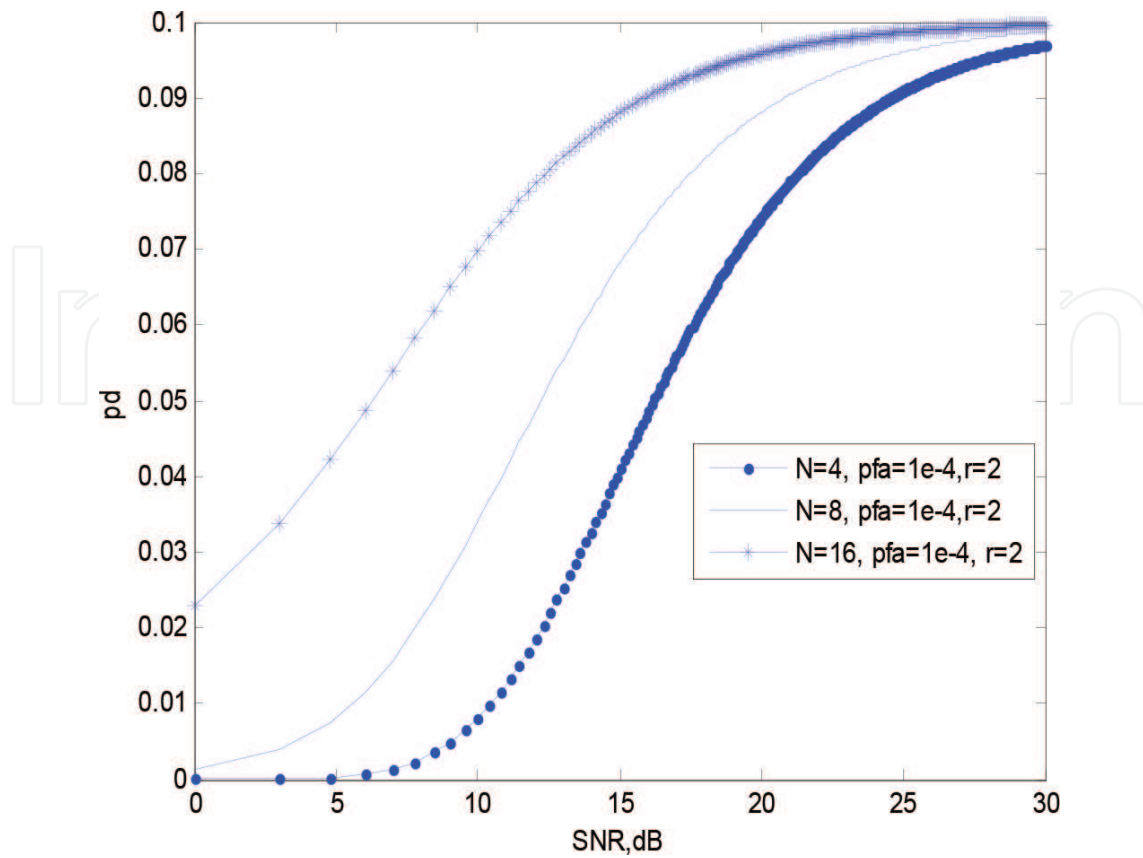


**Figure 14.** Performance of CA-CFAR at a non-homogeneous background (two interfering targets) with varying reference window and fixed  $P_{fa}$ .

where  $f(Z)$  and  $F(Z)$  are the PDF and CDF, respectively. For a homogeneous background,  $F_i = G(n, 2\mu')$ . The false alarm probability in this case is found by computing the moment generating function (MGF) of  $Z$  as follows:

$$M_z(T) = \int_0^\infty f_1(y)F_2(y)\exp(-Ty)dy + \int_0^\infty f_2(y)F_1(y)\exp(-Ty)dy = M1 + M2 \quad (37)$$

where

$$f_1(y) = \frac{\gamma_1^{-n}y^{n-1}\exp\left(-\frac{y}{\gamma_1}\right)}{(n-1)!} \quad (38)$$

$$f_2(y) = \frac{\gamma_2^{-n}y^{n-1}\exp\left(-\frac{y}{\gamma_2}\right)}{(n-1)!} \quad (39)$$

$$F_1(y) = 1 - \exp\left(-\frac{y}{\gamma_1}\right) \sum_{j=0}^{n-1} \left(\frac{y}{\gamma_1}\right)^j / j! \quad (40)$$

$$F_2(y) = 1 - \exp\left(-\frac{y}{\gamma_2}\right) \sum_{j=0}^{n-1} \left(\frac{y}{\gamma_2}\right)^j / j! \quad (41)$$

Substituting Eqs. (38)–(41) into Eq. (37) and after some algebraic manipulations, the following expression is obtained:

$$M_1 = (1 + \gamma_1 \check{T})^{-n} - \sum_{j=0}^{n-1} \binom{n+j-1}{j} \gamma_1^{-n} \gamma_2^{-j} \left\{ \frac{1}{\gamma_1} + \frac{1}{\gamma_2} + \check{T} \right\}^{-(n+j)} \quad (42)$$

$$M_2 = (1 + \gamma_2 \check{T})^{-n} - \sum_{j=0}^{n-1} \binom{n+j-1}{j} \gamma_2^{-n} \gamma_1^{-j} \left\{ \frac{1}{\gamma_1} + \frac{1}{\gamma_2} + \check{T} \right\}^{-(n+j)} \quad (43)$$

Exploiting the assumption that both sides of the window are of homogeneous clutter, we can see in Eqs. (42) and (43)  $\gamma_1 = \gamma_2$  therefore

$$P_{fa} = M_1 + M_2 = 2(1 + \check{T})^{-n} - 2 \sum_{j=0}^{n-1} \binom{n+j-1}{j} (2 + \check{T})^{-(n+j)} \quad (44)$$

The probability of detection for GO-CFAR is simply obtained by setting  $\check{T} = \frac{\check{T}}{s+1}$  in Eq. (44), that is,

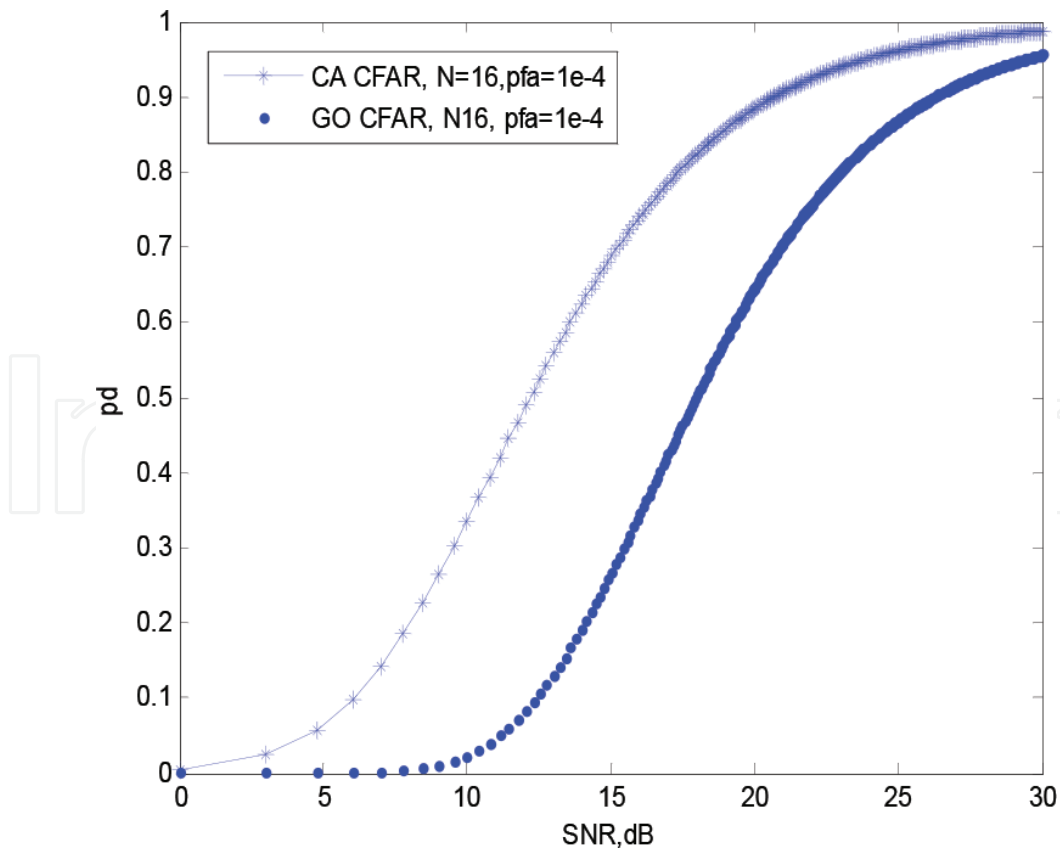


**Figure 15.** Performance of GO-CFAR compared to CA-CFAR when clutter background is homogeneous.

$$P_d = 2 \left( 1 + \frac{\check{T}}{S+1} \right)^{-n} - 2 \sum_{j=0}^{n-1} \binom{n+j-1}{j} \left( 2 + \frac{\check{T}}{S+1} \right)^{-(n+j)} \quad (45)$$

where  $\check{T}$  is the scale factor.

**Figure 15** shows the performance of GO-CFAR compared to that of CA-CFAR when the clutter background is homogeneous. It is clear that CA-CFAR outperforms GO-CFAR when both algorithms operate in homogeneous background.

The SO-CFAR is a modification of the CA-CFAR scheme so as to alleviate the problem of the presence of close spaced targets in the reference window. In the SO-CFAR scheme, the estimated power noise represents the smaller value of two sums  $Y_1$  and  $Y_2$ . That is [16]

$$Z = \min(Y_1, Y_2) \quad (46)$$

In this case, the PDF of  $Z$  is given as [Weiss]

$$f_z = f_1(Z)[1 - F_2(Z)] + f_2(Z)[1 - F_1(Z)] = f_1(Z) + f_2(Z) - [f_1(Z)F_2(Z) + f_2(Z)F_1(Z)] \quad (47)$$

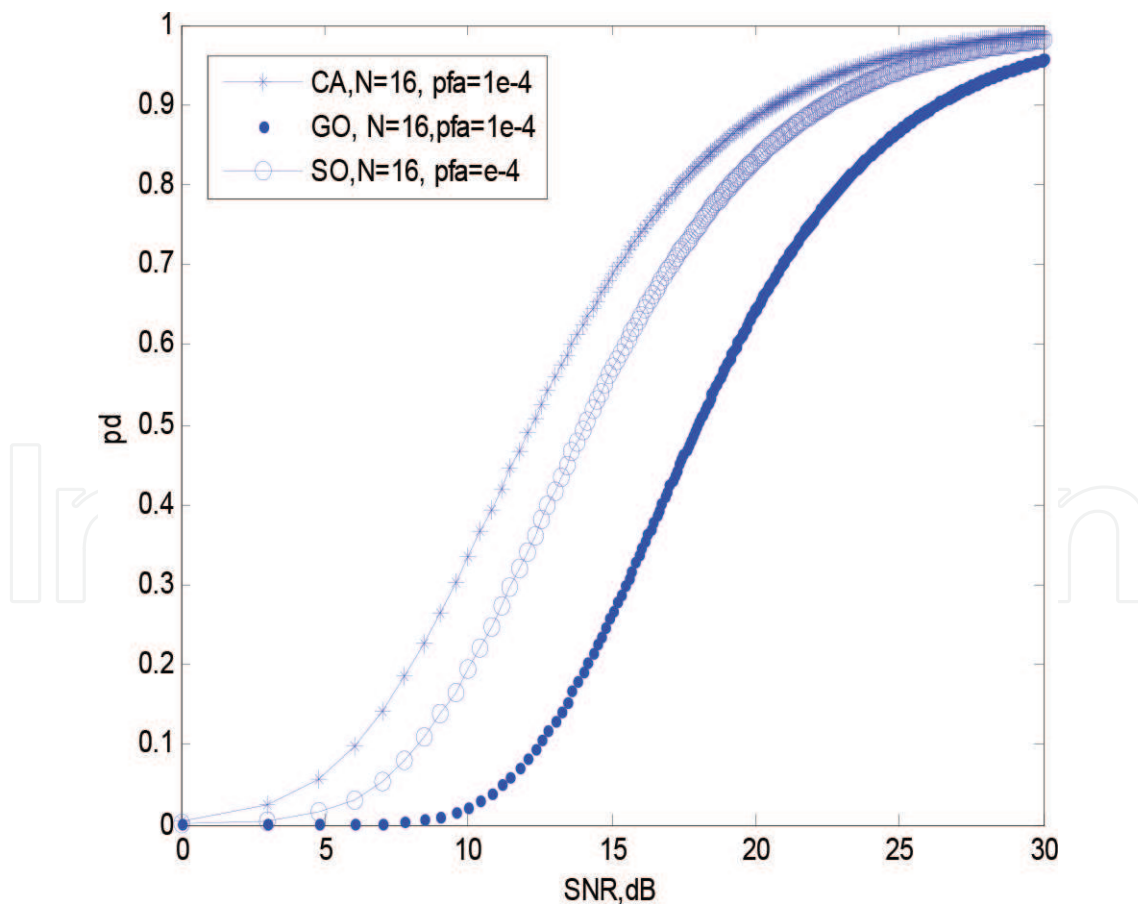


**Figure 16.** Performance comparison of the three processors (CA-, GO- and SO-CFARs) in the homogeneous background (Pfa = 1e-4).

The probability of SO-CFAR can be obtained by the MGF or

$$P_{fa-SO} = M_{Y1}\left(\frac{\check{T}}{2\mu'}\right) + M_{Y2}\left(\frac{\check{T}}{\mu'}\right) - P_{fa-GO} = 2 \sum_{j=0}^{n-1} \binom{n+j-1}{j} (2 + \check{T})^{-(n+j)} \quad (48)$$

The probability of detection for this scheme can be given by the setting  $\check{T} = \frac{\check{T}}{S+1}$ , that is,

$$P_{d-SO} = 2 \sum_{j=0}^{n-1} \binom{n+j-1}{j} \left(2 + \frac{\check{T}}{S+1}\right)^{-(n+j)} \quad (49)$$

**Figure 16** shows a performance comparison between CA-, GO- and SO-CFARs when the background is homogeneous. When the background of clutter is not homogeneous, that is, the reference window contains clutter edges or more than one target found in the reference window, this situation increases the false alarms when the processor is CFAR.

## Author details

Moutaman Mirghani Daffalla<sup>1\*</sup> and Ahmed Awad Babiker<sup>2</sup>

\*Address all correspondence to: mtnmir@gmail.com

1 Institute of Space Research and Aerospace (ISRA), Khartoum, Sudan

2 Engineering College, Karary University, Omdurman, Sudan

## References

- [1] Skolnik MI. Introduction to Radar Systems. 3rd ed. Boston: McGraw-Hill; 2001
- [2] Skolnik MI. Radar Handbook. New York: McGraw-Hill; 2008
- [3] Brookner E. Radar Technology. Dedham: Artech House Inc.; 1977
- [4] Mirghani M. Signal Analysis and Processing. Sudan: Communication and Navigation Research Center (CNRC), Karary University; 2012
- [5] Smith SW. The Scientist and Engineer's Guide to DSP. San Diego: California Technical Publishing; 1997
- [6] Mirghani M. Radar Principles. Sudan: Karary Academy of Technology; 2006
- [7] Mirghani M. Radar Signal Coding and Waveform Design. Lambert Academic Publishing. ISBN: 978-3-659-94632-5 2016
- [8] Mirghani M. Adaptive multifunction filter for radar signal processing. In: ICCEEE 2013, IEEE Conference, Khartoum; 2013

- [9] Haykin S. Adaptive Filter Theory. 4th ed. Upper Saddle: Prentice Hall; 2002
- [10] Haykin S, Widrow B. Least-Mean-Square Adaptive Filters. Hoboken: Wiley; 2003
- [11] Nathanson FE. Radar Design Principles, Signal Processing and the Environment. 2nd ed. New York: McGraw-Hill Inc.; 1991
- [12] Anderson JM. Nonlinear suppression of range ambiguity in pulse Doppler radar. PhD dissertation, Air Force Institute of Technology, Air University; 2001
- [13] Bell MR. Diversity and Adaptive Waveform Techniques for Pulse-Doppler Radar and SAR. Indiana: Purdue University; 2006
- [14] Rohling H. Radar CFAR thresholding in clutter and multiple target situations. IEEE Transaction on Aerospace and Electronic Systems. 1983;**AES-19**(4):608-618
- [15] Weis M. Analysis of some modified cell-averaging CFAR processors in multiple target situations. IEEE Transaction on Aerospace and Electronic Systems. 1982;**AES-18**(1):102-113
- [16] Gandhi PP, Kassam SA. Analysis of CFAR processors in non-homogeneous background. IEEE Transaction on Aerospace and Electronic Systems. 1988;**24**(4):427-444

IntechOpen

